Computational Method for Network Passive Software Robotic Devices

BY

TOMMASO CARELLA
B.S, Politecnico di Milano, Milan, Italy, 2016

THESIS

Submitted as partial fulfillment of the requirements
for the degree of Master of Science in Bioengineering
in the Graduate College of the
University of Illinois at Chicago, 2018

Chicago, Illinois

Defense Committee:

James L. Patton, Chair and Advisor

Max Berniker, Mechanical & Industrial Engineering

Elena De Momi, Politecnico di Milano

To my Grandfather, Cesare, who is no more among us.

I know that even where you are now you are still very proud of me.

ACKNOWLEDGMENTS

First and foremost, I would like to express my most sincere gratitude to Prof. Jim Patton, whose guidance and suggestions made this work possible, for giving me te opportunity to work and learn at the RoboticsLab and for investing financially on me in order to have me stay in Chicago for an additional semester.
Moreover, I would like to thank all the people from the MLB Lab; your help and advice has been very valuable to me and your friendship truly appreciated.

Many thanks to Judy and Dan West; you were not just hosts but a family to me: thank you for making me part of your family, for treating me as a nephew (not as a son, I know that you do not want to be parents anymore) and for making my experience in the United States so special. A particular mention to the young Gideon, it was very fun to have you around!
Thanks to all the people I met in these nine months in Chicago, especially to the *United Nations* group: I am very proud to have published my first paper with you.
Thanks to the *Casa Italia* group; my experience would not have been the same without you. A special mention goes to the *Unicorn Girls* and to my *Cavalieri*.

Thanks to all my *Gente Malata* and *Capodanno* friends: you are my second family and my life would be boring without you!

ACKNOWLEDGMENTS (continued)

Moreover, I want to thank Baro and the other friends from Politecnico for sharing never–ending classes with me.

The most important thanks to Giulia, I would not have been here without your help and your support; I know I am an anaffective person the most of the time, but I want to say that sharing with you this journey made it the best experience of my life.

Thanks to all my grandparents, Enrico, Raffaela and Anna for always supporting me and taking care of me, to my uncle, Chicco, and my aunt, Valentina, for helping me financially and for being always present. Moreover, a special mention also to the *Tradatesi* and to the growing Grazioli family.

Last but not least, thanks from the bottom of my heart to my parents, Fabio and Fabrizia; you made me the person I am now and the one I will become and I would never be able to express the gratitude I feel. Thank you, also, to my sisters Caterina, Benedetta and Sonya and my brother, Simone, for making my everyday life so special and full of meaning.

TC

TABLE OF CONTENTS

TABLE OF CONTENTS (continued)

CHAPTER **PAGE**

LIST OF TABLES

LIST OF FIGURES

LIST OF ABBREVIATIONS

ADLs	Activities of Daily Living
MIME	Mirror–Image Motion Enabler
DoF	Degrees of Freedom
MARIONET	Moment arm Adjustment for Remote Induction Of Net Effective Torque
SEA	Series Elastic Actuators
T–WREX	Therapy Wilmington Robotic Exoskeleton
CoR	Center of Rotation
TBM	Total Body Mass

SUMMARY

In the past years the number of people affected by stroke has grown dramatically, leading survivors to long–term disabilities in the 50% of the cases. To these people rehabilitation is the only possibility to achieve a total or, at least, partial recovery from their motor impairment.

In this context robotic rehabilitation has been developing greatly, contributing to the restoration of the functional capacity of high number of patients. Despite being a useful tool for recovery, mechanisms are bulky, uncomfortable for the patients and expensive, so that they are still not widely used in many cases during therapies. Furthermore, in a great variety of situations, the robot is utilized to move the arm of the patient in a passive way, wasting the great potential of these devices.

This work aims at developing a new inexpensive tool for rehabilitation, completely passive, composed only by elastic elements, such as springs, highly and simply customizable by a therapist and able to exert torque to the upper limbs of a patient; moreover, it will be able to achieve different kinds of therapies, based, for example, on the concept of error augmentation or gravity compensation.

In particular, this research concentrates on the development of an optimization algorithm able to find the set of optimal parameters needed for the customization of the system, performed according to a patient's specific motor deficits.

CHAPTER 1

INTRODUCTION

1.1 Motivation

1.1.1 Stroke survivors: a growing population

Stroke is the leading cause worldwide for what concerns long–term disability; in fact, one in 6 people in the world will experience stroke and ≈ 750000 people in the US are affected each year [1], with survival rate of the 82% [2]. Moreover, more than the 50% of the survivors will experience lasting disabilities [3] such as sensation loss, spasticity, imbalance strength, jerkiness, muscle coupling, poor planing and motion inaccuracies, leading to the inability to perform the so–called Activities of Daily Living (ADLs), a set of functional movements such as routine tasks of personal care, feeding or communicating [4]. Because of the aging of the population, the number of cases is destined to rise dramatically in the next years; recent statistics, in fact point out that only 10% of stroke patient are between the age of 18 and 50 [5]. Stroke generates an estimated expense of 33 billion dollars connected to not only the health care and lost days at work [1]; moreover, it results in a decreased quality of life not only for the patients and their families, but also for the caregivers [6][7][8][9].

For this growing population, rehabilitation is the process that aims to restore the maximum functional capacity possible and it is the only way for a patient, who presents residual disability, to improve his condition. Therapy should start at an early stage or, otherwise, the chances to obtain an acceptable recovery are reduced [10]. However, researchers have indicated that, even more than 6 months after the stroke (in the phase that is called chronic stage), there is the possibility to further motor recovery [11] [12], but, since insurances providers do not usually cover chronic patients' therapies and for the therapists working with them, the needed help to recover should be found somewhere else.

1.1.2 Robotic rehabilitation

In this context, machine–assisted therapy has been proven to be reasonable for enhancing physical outcomes for patients who suffered from neurological disabilities. In general, past research has been focusing on active robotic devices, in which the patient is physically guided by the robot itself in order to accomplish a specific movement and the therapist acts as a simple bystander. Some of these previous devices are the Mirror–Image Motion Enabler (MIME), a 6 Degrees of Freedom (DoF) end effector which applies forces in a certain direction so as to achieve the desired movement [13], and the InMotion2 (MIT MANUS), a 2 DoF robot that shows three different modalities for the user, among which the totally assisted movement procedure, in which the arm is moved passively [14].

Although devices such as the InMotion2 were shown to motivate patients to practice and to have a positive therapeutic advantage, subjects do not improve if the technology dominates movements [15] [16]; the main reason, as many researchers pointed out, is that, being guided completely by a robot, a patient can become lazy [17][18]. Moreover, robotic guidance machines are still expensive (for example, InMotion2 costs $\approx$ 100000\$). Finally, since stroke varies widely in effects and severity, it is problematic to treat patients in the same way.

From these problems the need to advance devices arises. They should be lightweight, low–cost, easy to operate and customizable. Moreover, in recent years simple exoskeletons for assistance, therapy and motor control have been developed: they involved passive elements, such as springs, which are able to generate desired torques [19][20].

1.2 Prior Studies

One attempt to find a solution to the aforementioned issues was done in our group with the Moment arm Adjustment for Remote Induction Of Net Effective Torque (MARIONET) [21] [22], a cable–driven device, which is able to deliver torque to a joint. This kind of design aims at controlling the generated torque through changes in the moment arm (Figure 1), whereas in most of the previous mechanisms, such as the String–Man[23], the moment exerted is a function of the cable tension.

1.2.1 MARIONET: first model

The first prototype of the MARIONET was part of the family of the so–called Series Elastic Actuators (SEA) mechanisms, which are formed by an elastic element in series with an actuator. The advantage of this kind of approach is that torque ripple, undesired errors and backlash are dampened, though some position accuracy and bandwidth are sacrificed as a result; the fundamental compliance of the SEAs is highly suitable for human–robot interactions [24]. The mechanism consisted of a rotator, actively controlled by a motor, and a passive link; a second motor worked as a tensioner. Despite not presenting springy components, the MARIONET

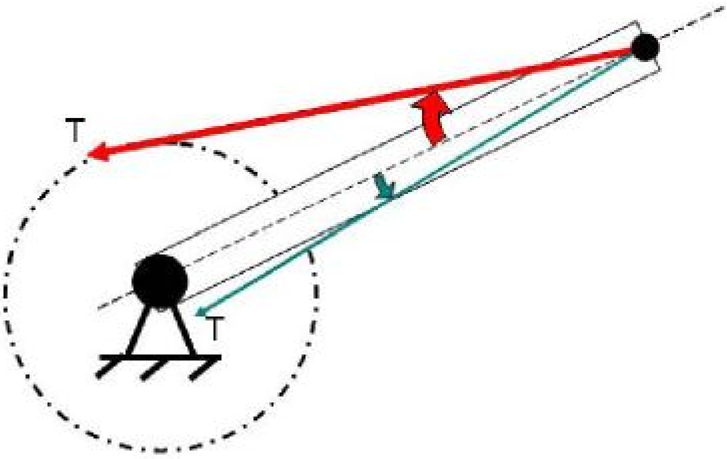

Figure 1: Torque controlled through changes in the moment arm: being equal the stiffness, a longer arm results in a higher torque (as pictured by the thicker *red* arrow); the *blue* one shows that a smaller arm produces a lower moment [22].

behaved exactly as a SEA, creating conservative force field generated via the tensioner. Although the system presented mechanical issues, connected mainly to friction, it managed to deliver torque to the desired joint with the convenience of remote actuation and independent control on equilibrium and compliance [21]. However, this version of the device was still a non–wearable, "heavy duty" robot.

1.2.2 MARIONET: at–home rehabilitation device

Whereas the first model was thought as a one–joint device, in the second generation the concept of the MARIONET was expanded so as to achieve an inexpensive two–joint machine for at–home rehabilitation [22]. Since it was developed as a tool for private use, the first issue to address was the user's safety, resulting in a device that presented low inertia and a low impedance with the interface, thanks to the use of SEAs; moreover, the actuator, being the heaviest part of the overall machine, was moved to the base of the device.

The design of this second prototype was divided into four different parts:

1. *Design for Function:* the two–joints system had to be a Manipulandum for upper extremities, highly customizable, so as to fit several users, and safe; furthermore, it had to be lightweight, inexpensive and mobile.
2. *Design with Cables:* the use of cables has some drawbacks, like the fact that they can wear out; therefore, the arrangement of the MARIONET aimed at avoiding process such as rope twisting, sharp augment in load, wrapping, etc.
3. *Design for Safety:* safety of the patient was the main concern; many possible failures modes where taken into account when designing the system, such as cable failure, electrical faults, etc., addressing each of them (cable guards, mechanical stops).
4. *Design for Control:* the MARIONET was controlled by four inputs: the position of the rotators (for every joint) and the motors acting as tensioners.

The most interesting aspect is that the device no longer needed rigid links, but, instead, the patient's arm itself was sufficient as a stiff element; moreover, since the MARIONET did not use elastic elements, cushioning came from the natural damping of the human arm, which showed to be more than enough to avoid instability [22]. Finally, it is important to point out that the system was suitable to to accomplish gravity compensation (section 1.2.3) and to exert both assistive and error enhancing forces, the latter being a new rehabilitation technique that will be addressed in section 1.2.4.

1.2.3 Gravity compensation

In order to improve rehabilitation techniques involving robots, many scientist focused on *gravity compensation* for the upper limbs. The aim is to compensate for the weight of the patient's arm, so as to augment their active range of motion[27]; in fact, as several studies showed, the working area of patients increased immediately during reaching tasks performed while providing gravity compensation with respect to unsupported movements [28]. In order to implement this method, the torque generated by the arm weight at each joint is calculated and compensated through the robot. One attempt to achieve gravity compensation was made by Sanchez et al. with the Therapy Wilmington Robotic Exoskeleton (T–WREX) [29] a passive, backdriveable, five DoF mechanism that counterbalanced the arm weight using elastic bands. This device was thought for at–home rehabilitation, thus presenting important safety constraints such as not generating power and the incapability to move on its own. Researchers demonstrated the ability to allow a larger range of motion, helping patients in performing ADLs. However, on the other hand, the system resulted in a more expensive device with respect to other devices on the market, and, moreover, it is only able to implement fixed levels of gravity support dependent on the number of elastic bands that are used.

1.2.4 Error augmentation

In recent years many scientists have speculated that a patient can learn more by dealing with large errors, since coordination in impaired subjects seems to benefit from the manipulation of this kind of inaccuracies [25]. This is linked to the neuroplasticity of the nervous system and to its adaptive nature.

This technique consists of isolation and selective augmentation of the error perceived by the patient in order to enhance learning. This can be achieved, for example, by applying a disturbance force to the subject or by giving a feedback smaller than the real one.

In this context, robots are able to exaggerate movements in real time during training by applying negative damping, viscosity or by setting an offset, for example, so as to increase the dynamic behaviour of the arm; the goal is to rise awareness of any deviation from the expected performance. The success of this technique might be due to different causes, such as patient's motivation or the fact that the damaged nervous system is not sensitive to small errors. However, there is not yet a complete understanding of the processes underlying this approach [26].

Therefore, there is the need for new rehabilitation tools that have to be customizable, lightweight and cheap. Moreover, these new systems should be able to exert torque without being actuated so as to avoid having a power source or electrical parts in order to be safe.

1.3 Objectives

Accordingly, this work aims at developing a new version of the MARIONET, a completely passive one, simplifying the actuators in order to use only elastic elements (such as diagonal springs), lightweight, versatile and cheap. Furthermore, this device should be highly customizable to match the characteristics and specific motor deficit of the patient (length of the arm, torque profile needed, etc.) and should be quickly assembled by a therapist.

Next, at a later time, we'll explore the possibility to stack a certain number of MARIONETs so as to achieve a more complex torque profile. EachMARIONET behaves as a basis function, like a truncated Fourier analysis or a radial basis function approximation, taking advantage of its intrinsic sinusoidal nature. The device could be used to fill in the gap of motor ability, to achieve *error augmentation*, or *gravity compensation*.

The main part of the work concentrates on computationally finding a set of optimal parameters for the stacked device, customizing it for the user through an optimization problem in MATLAB. Moreover, a two–joint MARIONET is studied, and the gravity compensation problem is addressed and solved to counterbalance the weight of the arm in the overall workspace. In Chapter 2 the methods will be addressed, while in Chapter 3 results will be shown and discussed; finally, in Chapter 4 conclusions on the work will be drawn.

CHAPTER 2

METHODS

2.1 MARIONET revisited: basic concepts

As stated in section 1.3, the new concept of the MARIONET involves a completely passive tool, formed by a pegboard to which a springy element is attached; there is no rigid link, since this part is substituted by the arm itself (Figure 2).

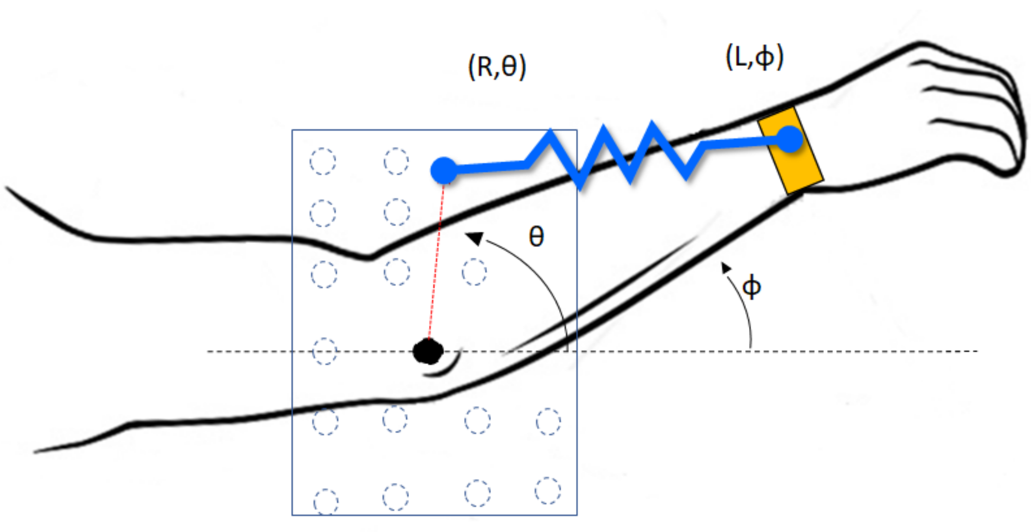

Figure 2: Basic concept of the MARIONET applied to the fore arm: R is the distance between the CoR and the point where the spring is attached, θ the angle between the horizontal and R, L is the arm length and ϕ is the angle between the horizontal and the arm.

2.1.1 Geometry

The geometry underlying the device is quite simple and is shown in Figure 3. Being R (in *yellow*) the distance between the Center of Rotation (CoR) (*green*) and the point where the spring is attached, θ the angle between R and the horizontal (dashed line), L (*black*) the length of the arm link and ϕ the one between L and the horizontal, the length of the spring L_s (*blue*) is:

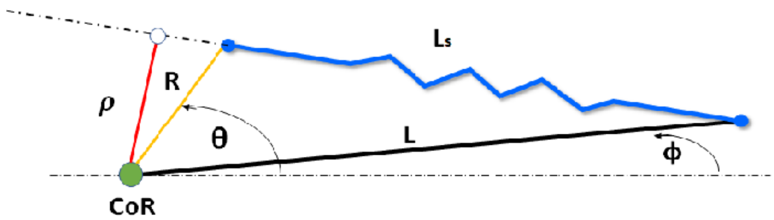

Figure 3: Diagram of the MARIONET.

$$L_s(\phi) = \sqrt{R^2 + L^2 - 2RL\cos(\theta - \phi)}. \tag{2.1}$$

In order to calculate the torque (τ) exerted by the device, the moment arm (ρ, *red* in Figure 3), which is a function of ϕ, since it varies as the angle changes:

$$\rho(\phi) = \frac{RL\sin(\theta - \phi)}{L_s}. \tag{2.2}$$

Therefore is possible to calculate the torque as:

$$\tau(\phi) = F_s \times \rho, \tag{2.3}$$

where F_s is the force calculated through Hook's Law, being k the stiffness of the spring and Δx the displacement of the elastic element, as:

$$F_s = -k\Delta x. \tag{2.4}$$

2.1.2 Single component torque profile

Figure 4 shows the torque generated by a single MARIONET, with $\theta = \frac{\pi}{3}$, $R = 0.1m$, the rest length of the spring $L_R = 0.1m$, the length of the fore arm $L = 0.26m$ and the stiffness $k = 250\frac{N}{m}$; its sinusoidal nature makes it suitable to act as a basis function and, so, a series of stacked elements can be used to achieve more complex torque shapes.

By varying only two parameters (R, θ), is it possible to achieve very different characteristics of these sinusoids, as displayed in Figure 5: the *blue* shape having the same parameters as before, the *red* one has $\theta = \frac{2\pi}{3}$ and same R, while the *green* one has $R = 0.05m$ and same θ.

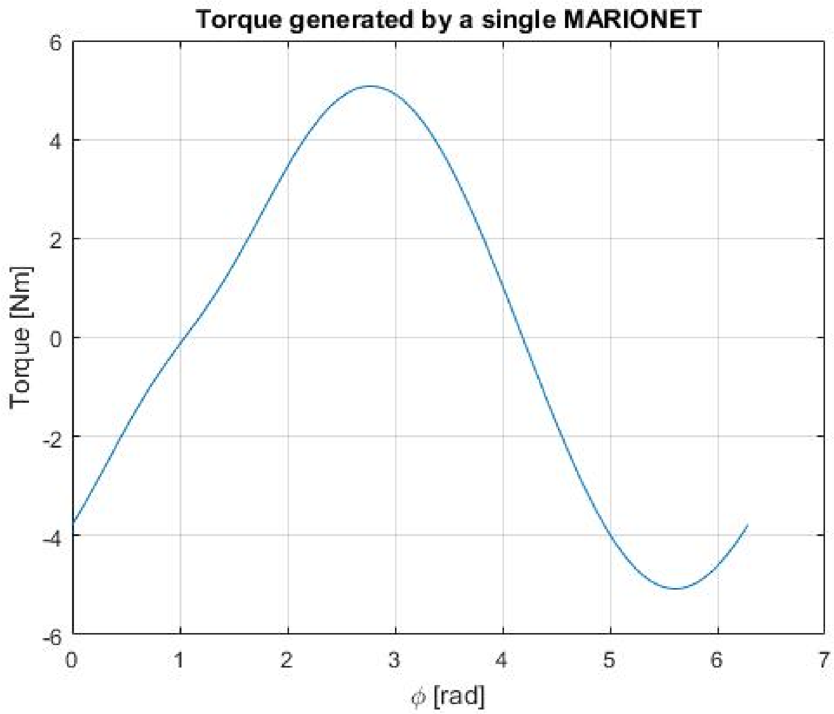

Figure 4: Torque generated by a single MARIONET in the range $[0, 2\pi]$. This males a nearly sinusoidal basis function that can be shaped and combined with others.

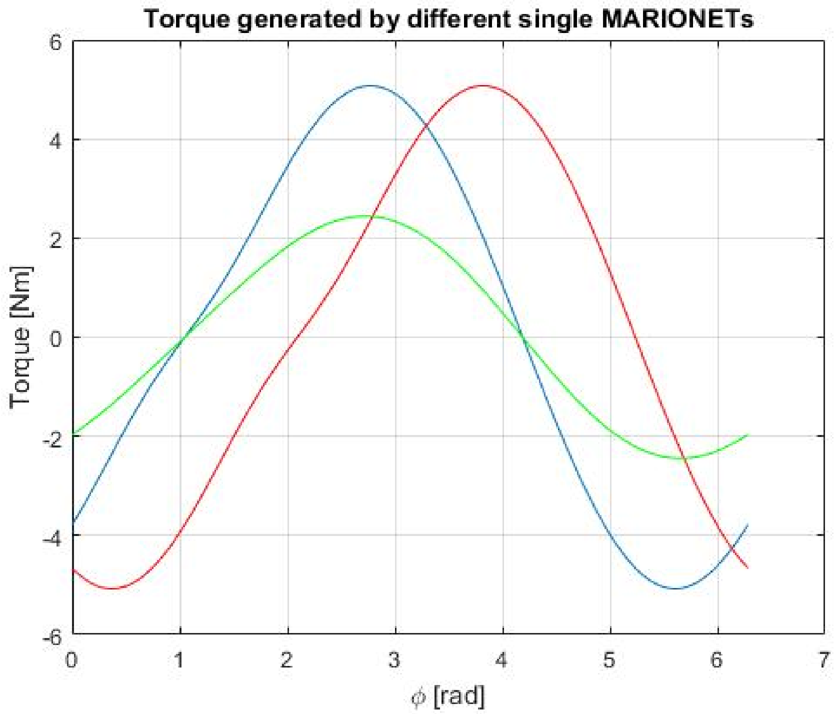

Figure 5: Torque generated by different single MARIONETs in the range $[0, 2\pi]$; varying parameters allows to have different sinusoids: for the *blue* profile $\theta = \frac{\pi}{3}$ and $R = 0.1m$, for the *red* one $\theta = \frac{2\pi}{3}$ and $R = 0.1m$ and for the *green* one $\theta = \frac{2\pi}{3}$ and $R = 0.05m$.

2.2 Stacking MARIONETs

As previously noted, stacking more and more elements can lead to the generation of complicated torque fields. In Figure 6, one possible solution for a multi–stacked elements configuration is shown.

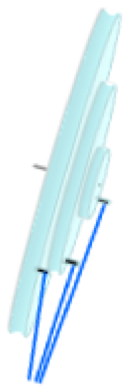

Figure 6: Concept of a 3–stacked elements configuration.

The total torque generated by the overall device is given by the sum of the moments generated by each one of the n single elements:

$$\tau_{tot} = \tau_1 + \tau_2 + ... + \tau_i + ... + \tau_n \tag{2.5}$$

Figure 7 shows the torque generated by three different MARIONETs (in *black*); as previously stated, a unique torque profile can be obtained, so as to achieve a specific task.

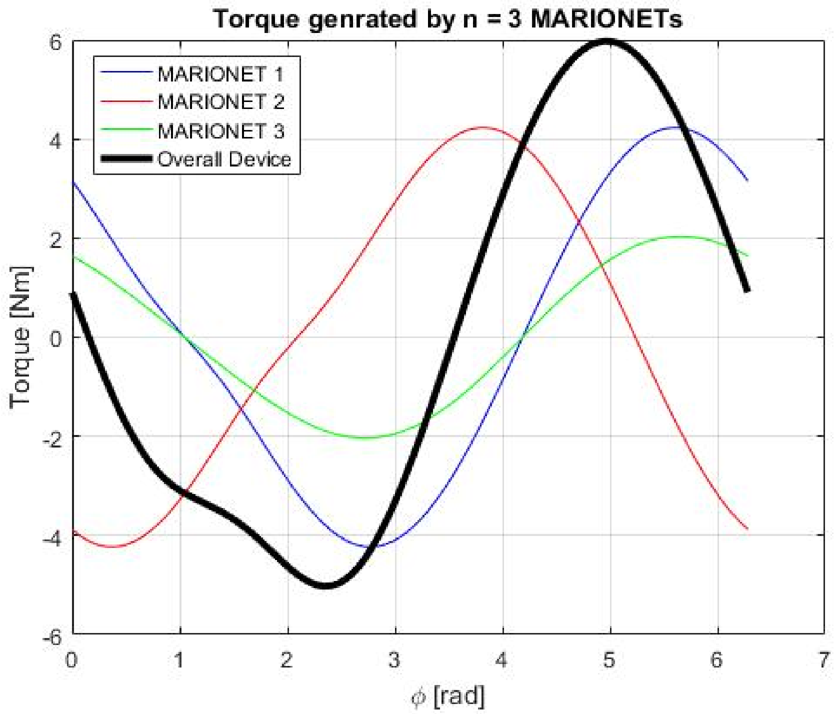

Figure 7: Overall torque generated by the sum of MARIONETs.

2.3 Two–joints MARIONET

An additional version of the MARIONET can be conceived linking directly the shoulder and the wrist through a spring, therefore obtaining a two–joints device. The scheme of the mechanism is reported in Figure 8.

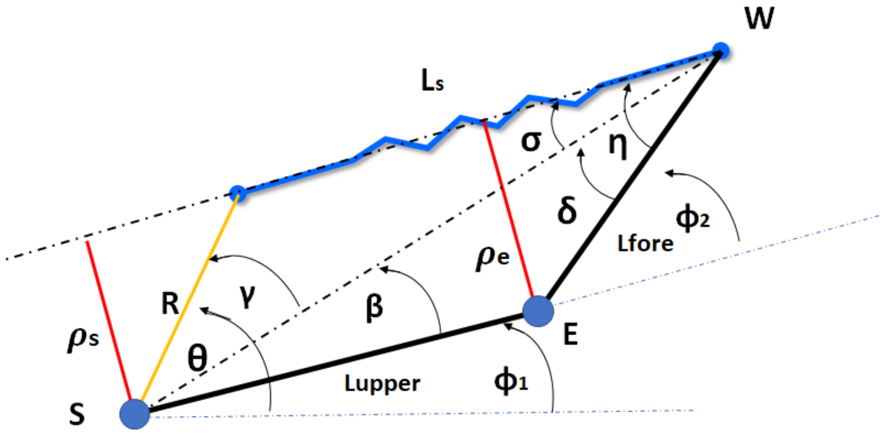

Figure 8: Diagram of the two–joints MARIONET.

First of all, the length of the spring L_s is calculated as:

$$L_s = \sqrt{\left(\frac{L_{fore}\sin(\phi_2)}{\sin(\beta)}\right)^2 + R^2 - \left(\frac{L_{fore}\sin(\phi_2)}{\sin(\beta)}\right) R\cos(\gamma)}, \tag{2.6}$$

where $\gamma = \theta - \beta - \phi_1$ and β represents the angle between L_{upper} and the diagonal of the quadrilateral composed by L_{upper}, L_{fore}, L_s and R (*black* dotted line) and is calculated using the *atan2* MATLAB function.

Then, the moment arm at the shoulder joint ρ_s is calculated:

$$\rho_s = \frac{\left(\frac{L_{fore}\sin(\phi_2)}{\sin(\beta)}\right) R\sin(\gamma)}{L_s}. \tag{2.7}$$

On the other hand, the moment arm at the elbow ρ_e is computed as:

$$\rho_e = L_{fore} \sin(\eta), \tag{2.8}$$

where $\eta = \delta + \sigma$, which are defined as:

$$\delta = \arcsin\left(\frac{L_{upper} \sin(\beta)}{L_{fore}}\right), \tag{2.9}$$

$$\sigma = \arcsin\left(\frac{R \sin(\gamma)}{L_s}\right), \tag{2.10}$$

Knowing ρ_s and ρ_e, the torques can be calculated using Equation 2.3.

2.4 Empirical optimization

Now that the geometrical basis are set, we aim at replicating every torque needed by a certain patient for rehabilitation purposes. Therefore, each MARIONET has to be tuned according to certain parameters that we are determined to find through the solution of an optimization problem; the algorithm, which will be explained in the next paragraphs, can be set to find two or three *optimal parameters* for each element. Of course, the higher the number of stacked MARIONETs and, as a consequence, the higher the number of parameters to be found, the higher the computational cost and the time spent processing.

2.4.1 Parameters

The two main parameters that the algorithm aims to find are R and θ (as represented in Figure 2); the former is the distance between the CoR and the point on the pegboard where the spring is attached, while the latter is the angle between the horizontal line and R. Moreover, as pointed out before, a third parameter can be addressed: the stiffness of the elastic element k. The first two parameters have an impact on the length of the moment arm (as expressed by Equation 2.2), while the third one acts on the force exerted by the spring.

2.4.2 Code description

Figure 9 shows the flow chart of the MATLAB code that was developed in order to find the optimal parameters.

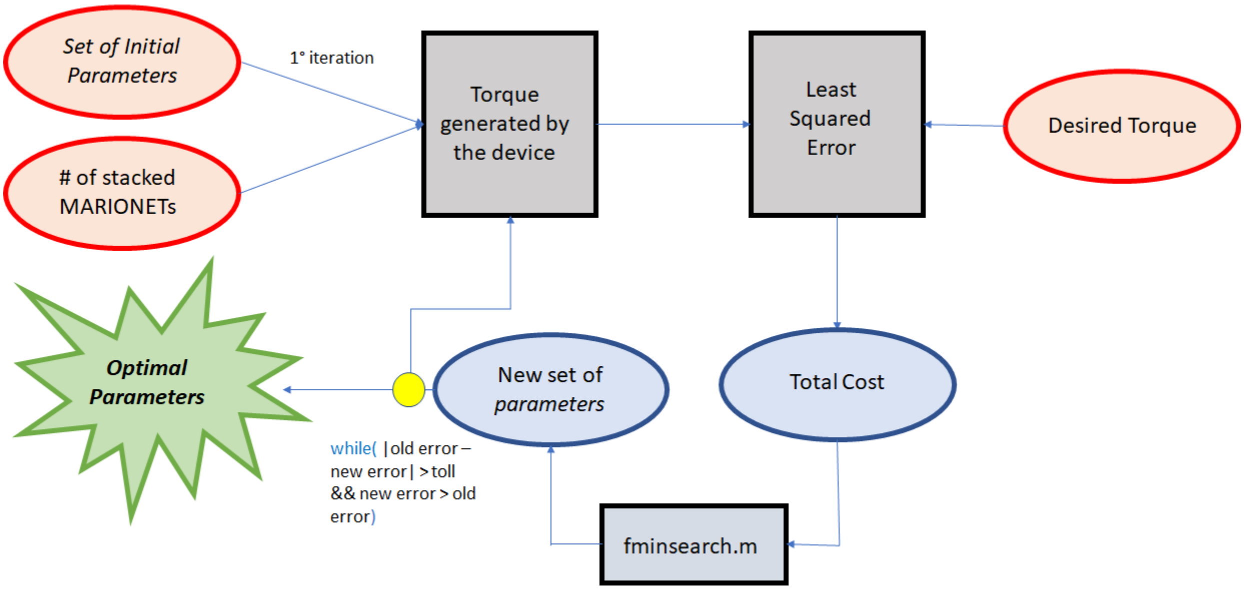

Figure 9: Flow chart of the developed MATLAB code: here are all the step implemented in order to find the optimal solution.

2.4.2.1 Inputs

There are three main *inputs* to the function (*red* ovals):

- *Number of stacked MARIONETs (N):* the number of different elements that we want to combine in order to obtain the desired torque.
- *Set of initials parameters:* Being M the number of parameters for each element, a $M \times N$ vector is created; this vector is thus filled in with random numbers thanks to the *rand* function.
- *Desired torque:* The torque profile the patient needs for rehabilitation.

The initial overall torque (τ_{tot}) is calculated by using Equation 2.3 with the starting random parameters for each MARIONET and by summing all the obtained moments as in Equation 2.5.

2.4.2.2 Cost calculation

The chosen cost function for the optimization algorithm is the *Least Squared Error*, as defined by:

$$Cost = \sum_{1}^{n}(\tau_{tot} - Desired\ Torque)^2, \tag{2.11}$$

being n the length of the *Desired Torque* vector. Furthermore, since the device should be built for the patient to be comfortable, some restriction to the parameters are set. These were employed as regularization terms, or soft constraints. Of course, the R can not be negative and, in addition, its length its expected to be no longer than $0.1m$, since we want the patient to feel comfortable while wearing the device and a big mechanism would not accomplish such a requirement. For any $R < 0m$ and $R > 0.1m$ a *penalty function* was added, increasing the overall total cost. Moreover, some constraints are also applied to the stiffness of the elastic elements, when considered as a parameter in the optimization process; therefore, the cost increases when $k < 0$ or $k > 1000$. For both R and k, the cost was augmented by summing a penalty parameter multiplied by a certain factor measuring the violation of the constraints:

$$PenaltyFunction = |Param - Param_0|^3 \times 10^{15}, \tag{2.12}$$

where *Param* is the parameter under review and $Param_0$ is the inferior or superior limit for the parameter itself.

On the other hand, no penalty is needed for θ, since this angle is used in a periodic function.

2.4.2.3 fminsearch.m

This function, that is part of the *Optimization Toolbox* on MATLAB, is able to solve nonlinear problems using a derivative–free method; it aims to minimize a given function, that, in this case, is the total cost as defined in section 2.4.2.2. Therefore, it is able to find the optimal parameters that correspond to a local minimum [30]. The options where changed so as to have the highest number of iteration and evaluation of the function possible. Eventually, the output of this function is a new set of parameters, with which the new MARIONET torque is calculated.

2.4.2.4 "While" loop

One iteration of the code is not enough to obtain satisfying outcomes, so an outer *while* loop is added. This is to assure that a more global optima is found. The *while* loop presents two main condition and a third optional one:

- $|meanError_i - meanError_{i-1}| > toll$: if at the i^{th} step, the difference between the average error at i^{th} and $i-1^{th}$ is bigger than a certain tolerance (*toll*, to be decided), then loop is repeated; the average error is calculated as the mean of the difference between the MARIONET torque and the desired one.
- $meanError_i > meanError_{i-1}$ if the mean error calculated at the i^{th} step is bigger than the error at the previous one, then the loop continues.

In order to leave the *while* loop, these two conditions must be false at the same time (logical OR); moreover, a third one can be added:

- *number of iterations* $>$ *MaxIter*: this condition is added to avoid the code to get stuck; so, when the number of iterations i is bigger than a certain predetermined threshold (*MaxIter*), the *while* loop is left (being this condition linked with a logical AND to the previous two).

2.4.2.5 Optimal Parameters

When the *while* loop terminates, this means that the global *optimal parameters* have been found. These can be used to tune the different MARIONETs that are included in the device so as to achieve the torque needed by the patient.

2.5 Gravity compensation

In order to achieve gravity compensation, as defined in section 1.2.3, the first step is to find the torques needed to balance the moment generated by the arm weight; to do so, the free–body diagram of the human arm is studied. These torques are calculated under the condition of static equilibrium; moreover, the problem was simplified applying the weights of each part composing the arm at the middle point of each link, while the weight of the hand was applied at the wrist joint. Figure 10 shows the free–body diagram taken as a reference: ϕ_1 is the angle between the horizontal line and the SE segment, ϕ_2 the one between SE and EW links, τ_s and τ_e the torques to be found at shoulder and elbow joint respectively; in addition, the aforementioned weights are shown.

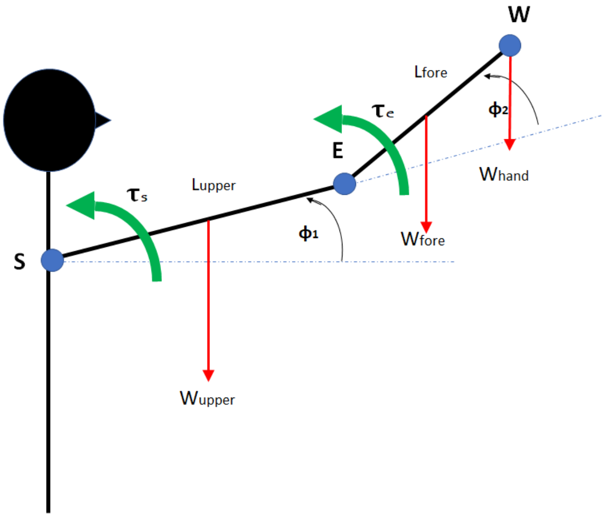

Figure 10: Free–body diagram used to calculate the torque needed for gravity compensation.

First of all, the mass of different parts of the arm is calculated as related to the Total Body Mass (TBM), as suggested by De Leva [31], and multiplied by the gravity acceleration ($g = 9.81\frac{m}{s^2}$):

- *Upper arm weight:*

$$W_{upper} = 2.71\% \times TBM \times g. \tag{2.13}$$

- *Fore arm weight:*

$$W_{fore} = 1.62\% \times TBM \times g. \tag{2.14}$$

- *Hand weight:*

$$W_{hand} = 0.61\% \times TBM \times g. \tag{2.15}$$

Solving the static problem as depicted in Figure 10, the torques needed to compensate for the moment due to arm weight are:

$$\begin{cases} \tau_e = (\frac{W_{fore}}{2} + W_{hand}) L_{fore} \cos(\phi_1 + \phi_2) \\ \tau_s = (\frac{W_{upper}}{2} + W_{fore} + W_{hand}) L_{upper} cos(\phi_1) + \tau_e \end{cases} \tag{2.16}$$

Moreover, knowing the torques, it is possible to represent them as force thanks to the *Jacobian matrix* (J), defined as:

$$J = \begin{bmatrix} -L_{upper}\sin(\phi_1) - L_{fore}\sin(\phi_1 + \phi_2) & -L_{fore}\sin(\phi_1 + \phi_2) \\ L_{upper}\cos(\phi_1) + L_{fore}\cos(\phi_1 + \phi_2) & L_{fore}\cos(\phi_1 + \phi_2) \end{bmatrix} \tag{2.17}$$

Now, the x and y components of F can be evaluated as:

$$\begin{bmatrix} F_x \\ F_y \end{bmatrix} = (J^T)^{-1} \times \begin{bmatrix} \tau_s \\ \tau_e \end{bmatrix} \tag{2.18}$$

Figure 11 shows the new representation of the torques needed to counterbalance the gravity; the corresponding force F (*green*) is given by the computed x and y components and is applied at the wrist. F is the force needed to compensate the moment generated by the arm weight, therefore it produces the equivalent effect as τ_s and τ_e together.

Now, thanks to the previous description it is possible to display all Forces needed to compensate the arm weight in a vector field (Figure 12); the aim is to find the parameters that can optimally match the torques needed in the overall space.

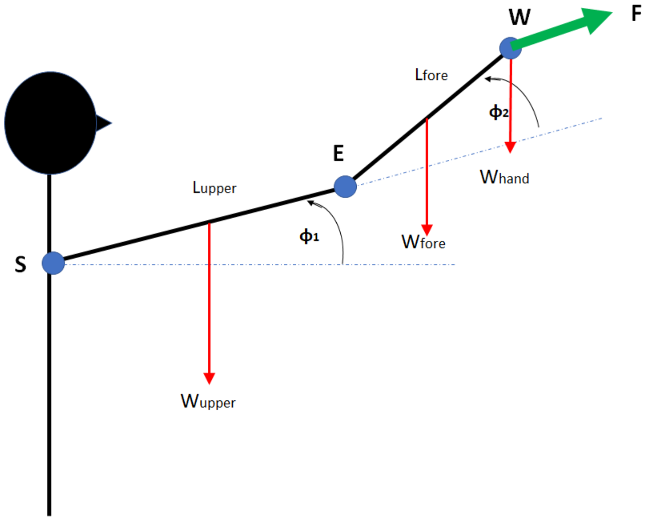

Figure 11: Free–body diagram that represents the torques as a force (F), as calculated through Equation 2.18.

In order to achieve accurate gravity compensation we show progressively more complex MARIONET combinations:

- The first one is developed using two different device, one applied from shoulder joint to the elbow, while the other from elbow to wrist.
- The second is expected to require only one device, connecting the shoulder joint directly to wrist.

Both this solutions are based on the previously described algorithms (the two–parameter form), even if the calculation of the *Cost Function* changes with respect to the original form.

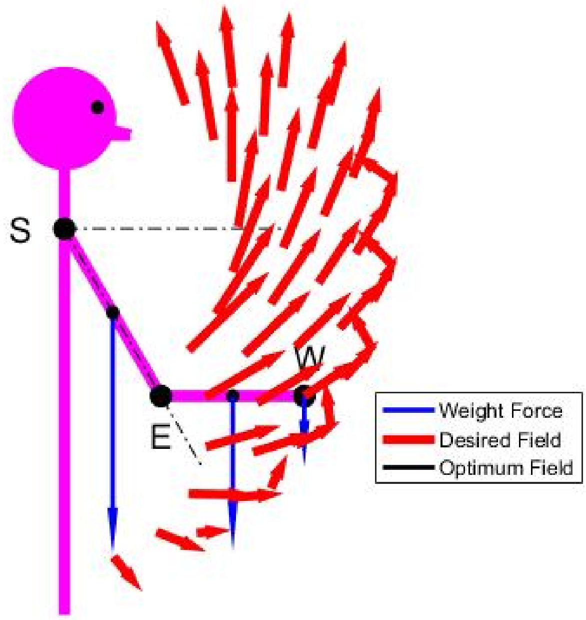

Figure 12: Vector field: each *red* arrow is the force at a certain shoulder–elbow angle couple able to compensate weight.

2.5.0.1 One-joint solution

The first method final objective is to find two different sets of parameters, one for each device, that, when given to the developed model, would be able to approximate the desired torques across the workspace; in order to do so, the calculation of the *cost function* had to undergo some changes. In fact, there was not just one profile to be estimated, but a series of different torques to be evaluated across the workspace, each of them corresponding to a point in the ϕ_1–ϕ_2 space (shoulder and elbow angles). Therefore, the cost could not be calculated as the mere least squared errors between the device torque and one target torque, but it must be computed as the sum of the least squared errors throughout the space, for both the shoulder and elbow:

$$TotalCost_{elbow} = \sum_{i=1}^{N_{angles}} \sum_{1}^{n} (\tau_{tot} - DesiredTorque_i)^2, \tag{2.19}$$

$$TotalCost_{shoulder} = \sum_{i=1}^{N_{angles}} \sum_{1}^{n} (\tau_{tot} - DesiredTorque_i)^2, \tag{2.20}$$

Where N_{angles} is the number of elements in which the ϕ_1 and ϕ_2 ranges are divided.

In this way it is possible to find the two optimal sets of parameters so as to have the best match in all the comprehensive gravity field. The target torques for the elbow joint are calculated by fixing one shoulder angle (ϕ_1) at a time, while varying the elbow one (ϕ_2) as presented in Figure 13a; on the other hand, the desired shoulder torques are obtained by fixing the elbow angle and altering the shoulder one (Figure 13b).

Eventually, the torques at the shoulder and at the elbow will be converted in forces using Equation 2.18 and will be scaled depending on the maximum force in the space (taking into account desired and optimal forces at the same time) according to Equation 2.21:

$$ScaledForce = \frac{Force}{MaxForce} \times 0.15. \tag{2.21}$$

Since for certain $\phi_1 - \phi_2$ combinations the $JacobianMatrix$ happens to be singular, the $MaxForce$ can become infinite, hence making it impossible to have a good representation of the vector

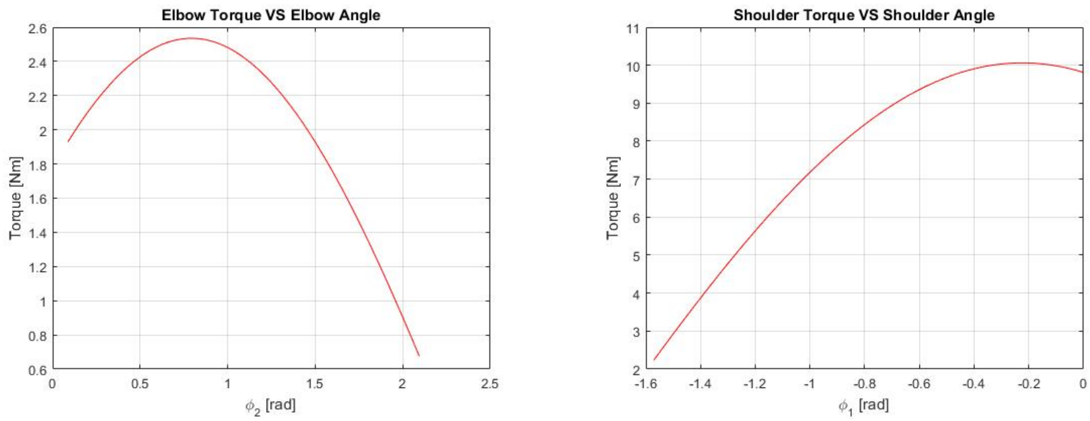

(a) Elbow torque profile obtained with a fixed shoulder angle $\phi_1 = -0.7933rad$

(b) Shoulder torque profile obtained with a fixed elbow angle $\phi_2 = 1.0807rad$

Figure 13: Elbow and Shoulder torque needed in order to compensate for gravity for fixed ϕ_1 and ϕ_2 respectively.

field; therefore, the points in which the matrix becomes singular are not taken into account.

2.5.0.2 Two-joint solution

The second solution, as previously explained, aims at approximating the torques able to compensate for the gravity using only one device connecting the shoulder with the wrist; the targets are the same ones shown in Figure 13 for the elbow joint, while the one for the shoulder, in this case, is computed fixing the shoulder angle and varying the elbow one, as Figure 14 shows.

In order to compute the set of optimal parameters, the cost function is calculated in the same way as before but for the fact that both the least squared errors evaluated on τ_s and τ_e are

Figure 14: Target torque at the shoulder for the two–joints version.

taken into account at the same time, therefore summing them in a unique total cost. So, the optimization algorithm has to minimize at the same time the costs from the shoulder and elbow joints:

$$TotalCost_{elbow} = \sum_{i=1}^{N_{angles}} \sum_{1}^{n} (\tau_{tot} - DesiredTorque_i)^2, \tag{2.22}$$

$$TotalCost_{shoulder} = \sum_{i=1}^{N_{angles}} \sum_{1}^{n} (\tau_{tot} - DesiredTorque_i)^2, \tag{2.23}$$

$$TotalCost_{overall} = TotalCost_{shoulder} + TotalCost_{elbow}. \tag{2.24}$$

CHAPTER 3

RESULTS AND DISCUSSION

First, the results of the optimization algorithm are shown, both with two and three *parameters* for each stacked element. Then, the conclusions on the gravity compensation process are illustrated.

3.1 Optimization results

In this section, the results of the two and three parameters problems are presented, focusing in addition on some complications connected to the way in which the algorithm is conceived; eventually a discussion on the optimal number of stacked elements is delineated.

3.1.1 Two Parameters

The first case is meant to demonstrate the process in the simplest manner; an elbow device is taken into account and the chosen parameters are R and θ; other quantities that is important to point out, set manually by the user, are the stiffness $k = 500\frac{N}{m}$, the length of the fore arm $L_{fore} = 0.26m$, the length of the spring in resting conditions $L_0 = 0.1m$ and the number of stacked elements $N = 5$ (resulting in a total of $M = 10$ parameters to be found). The desired torque was created to obtain an arbitrary sinusoidal shape.

By stacking 5 different MARIONETs (Figure 15, in *blue*) it is possible to approximate the target (*red*). The error, defined as the difference between the target and the exerted torque, is pictured.

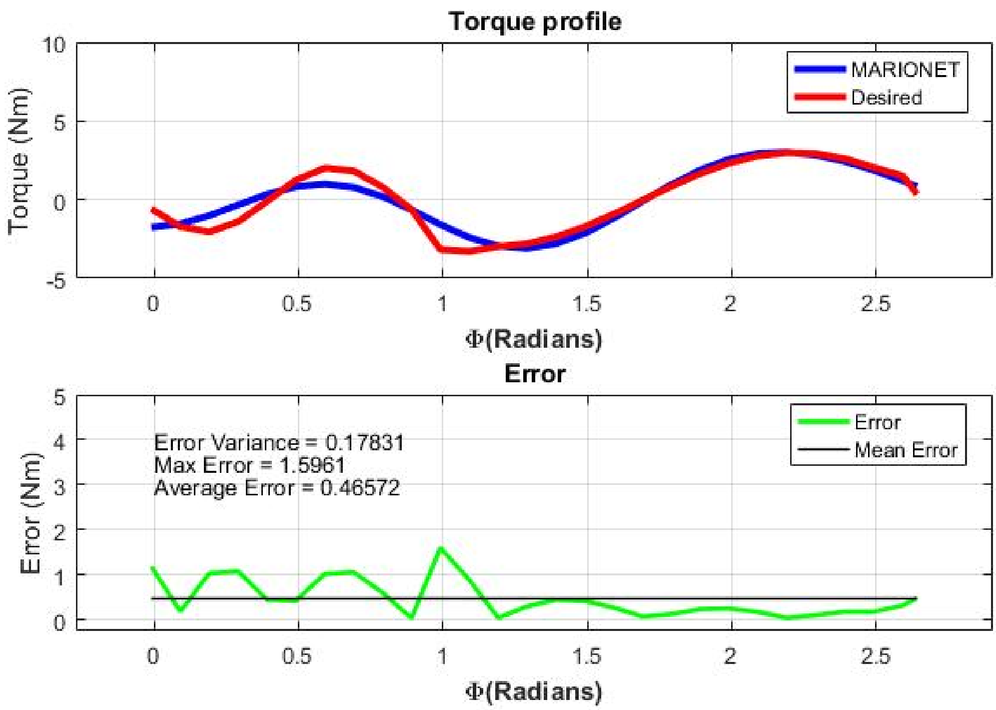

Figure 15: Top: in *blue* the torque generated by 5 MARIONETs, in *red* the target one. Bottom: the error (in *green*), calculated as the difference between the red and blue profiles, and the average error (*black* line); moreover, some information about the error are shown.

The *blue* shape is obtained with the parameters listed in Table I (which are different from the starting guess), in Figure 16 the arrangement of the MARIONETs is pictured and in Figure 17 each single component is shown.

TABLE I: OPTIMAL PARAMETERS FOR EACH SINGLE COMPONENT.

	R[m]	$\theta[rad]$
MARIONET1	0.1000	0.9407
MARIONET2	0.1000	3.2715
MARIONET3	0.1000	-1.5443
MARIONET4	0.1000	-0.3755
MARIONET5	0.0878	2.2786

An average error of $0.4657Nm$ was obtained in this case, with a variance $\sigma^2 = 0.17831$. Furthermore, it presents an average percentage error of $\approx 54\%$, which may seem high, but it is probably due to the fact that the target profile had sharp changes, which is difficult to replicate with sinusoidal functions. In order to prove this thesis, a smoother target torque profile was used,; in this case, the algorithm was able to achieve an average error of $0.0717Nm$ with a variance $\sigma^2 = 0.0028$ and the average percentage error is only 1.3087%. In fact, from Figure 18 it is possible to see that the two torques were almost completely overlapped, while the error was nearly null everywhere.

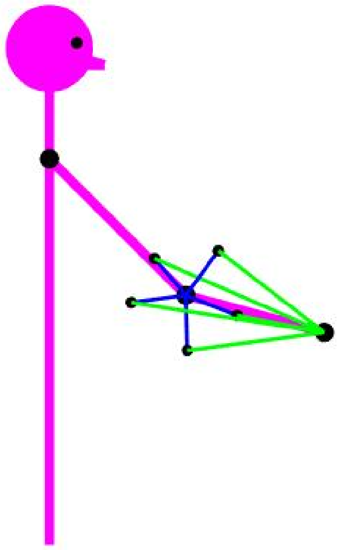

Figure 16: How the MARIONETs are arranged in the space: in *blue* is the parameter R and in *green* is the spring.

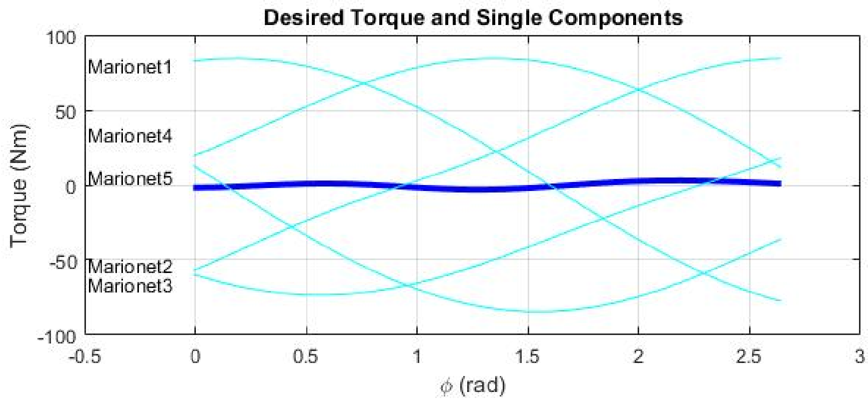

Figure 17: Top: in *blue* the overall torque generated by 5 MARIONETs is represented , while in *cyan* each single component is pictured.

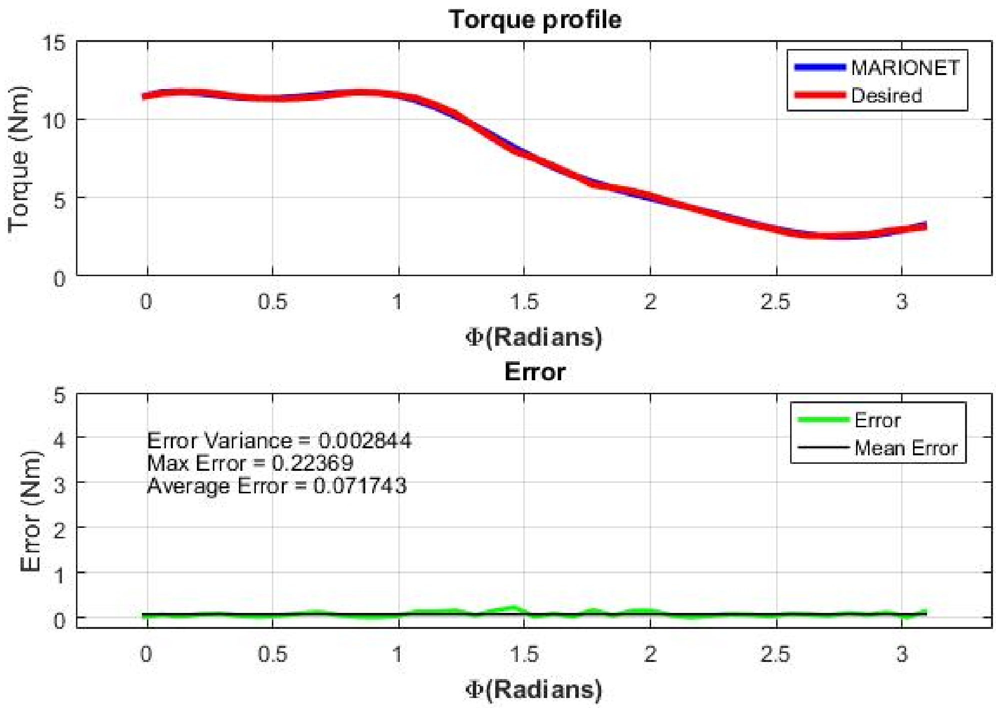

Figure 18: Results obtained with a smoother target torque. *Top*: the two torque fields were almost completely overlapped. *Bottom*: A smoother target resulted in smaller errors.

3.1.2 Three Parameters

Considerations made in sections 3.1.1 and 3.1.3 were still valid when adding a third parameter for each stacked MARIONET, which is(section 2.4.1), the stiffness k of the each spring. Having more variables to work on, this adaptation of the algorithm was better.

Average error was slightly lower than the one in Figure 15 (Figure 19 shows the results), with a value of 0.42417 (corresponding to a 43.6986% percentage error). In Table II, the obtained parameters are reported.

TABLE II: OPTIMAL PARAMETERS FOR EACH SINGLE COMPONENT.

	R[m]	$\theta[rad]$	$k[\frac{N}{m}]$
MARIONET1	0.10	-5.3266	533
MARIONET2	0.10	-0.5275	1000
MARIONET3	0.10	2.9027	50
MARIONET4	0.07	3.8921	1000
MARIONET5	0.09	3.7753	1000

The drawback of this version of the algorithm, obviously, is that the computational weight and time to process increased. Considering that the error calculated through this method did not decrease so dramatically and that the achieved results are almost the same, it seems unproductive to spend more resources using this version of the algorithm instead of the original.

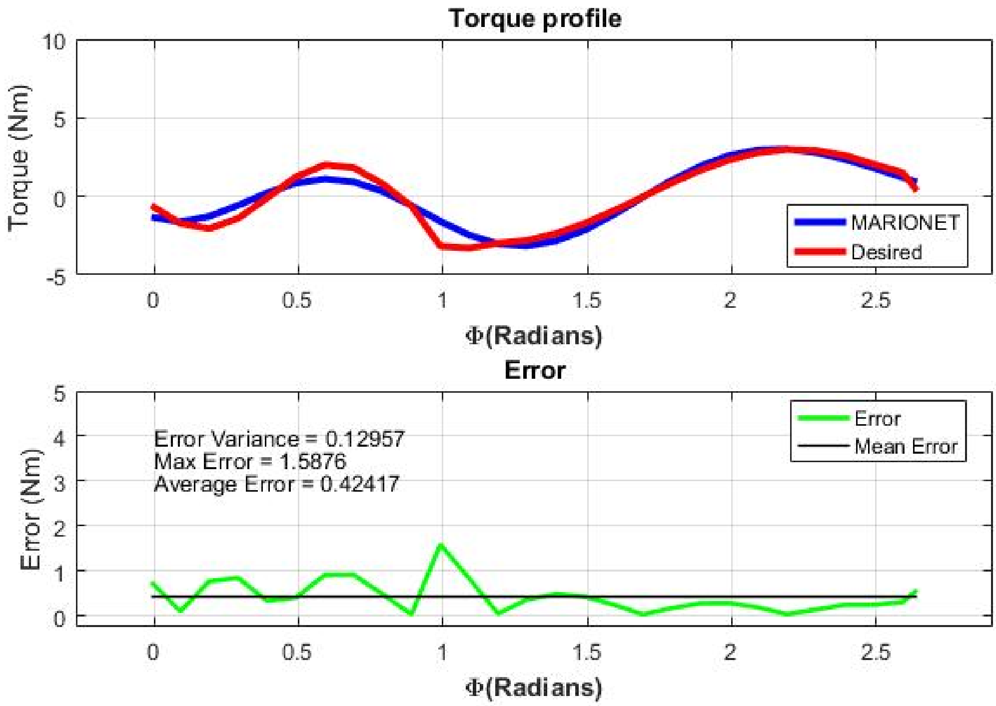

Figure 19: Top: in *blue* the torque generated by 5 MARIONETs, each tuned according to three parameters R, θ and k, in *red* the target one. Bottom: the error (in *green*), calculated as the difference between the red and blue profiles, and the average error (*black* line); moreover, some information about the error is shown.

3.1.3 How many stacked MARIONETs?

As more and more MARIONETs were stacked, the smaller the error got. We tested it (Figure 20); average error decreased less as the number of stacked elements increased. The error passed from $1.7721 Nm$ with only one MARIONET to $0.3169 Nm$ with ten. After five or six stacked elements the results approached a *plateau* and the decrease in error became small. These results were obtained solving the optimization problem with two parameters for each stacked element, with the same data and target profile reported in section 3.1.1.

In Table III all the errors are reported.

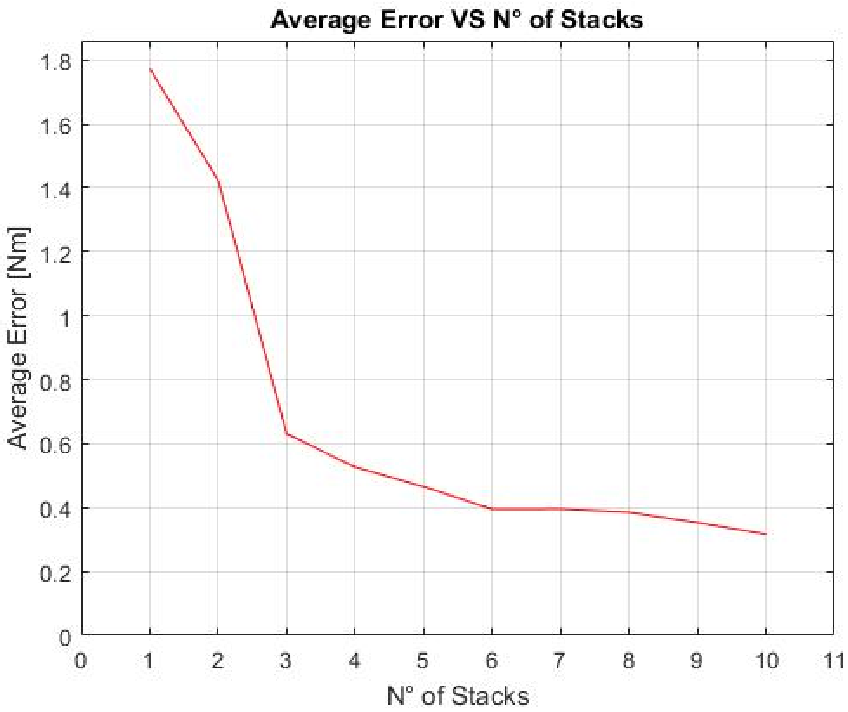

Figure 20: Trend of the average error with respect to the the number of stacked elements.

Since patients need to feel comfortable wearing the device, the number of MARIONETs composing the mechanism can not be too high. Moreover, a high number of components would result in an increased computational cost and time. This trade–off between error and complexity

TABLE III: AVERAGE ERROR [Nm] WITH RESPECT TO THE NUMBER OF STACKED ELEMENTS.

Stacked MARIONETs	Average Error [Nm]	Stacked MARIONETs	Average Error [Nm]
1	1.7721	6	0.3951
2	1.4225	7	0.3958
3	0.6304	8	0.3855
4	0.5263	9	0.3528
5	0.4653	10	0.3169

seems to be the point where the *plateau* starts, so choosing a five element solution appears to be optimal.

3.1.4 Problems connected to random initialization

Since the optimization algorithm starts with a random guess for the initial parameters, some concerns are to be addressed. In fact, the results of the process highly depend on the starting point.

A way to overcome this problem was developed: Figure 21 shows the method adopted. The optimization algorithm previously developed was inserted into a *"for"* loop whose number of iteration N_{iter} has to be decided by the user; at each iteration i, a set of optimal parameters is found, the average error is calculated and compared to the minimum mean error previously found. Eventually, when $i > N_{iter}$, the set of parameters corresponding to the minimum average error is taken.

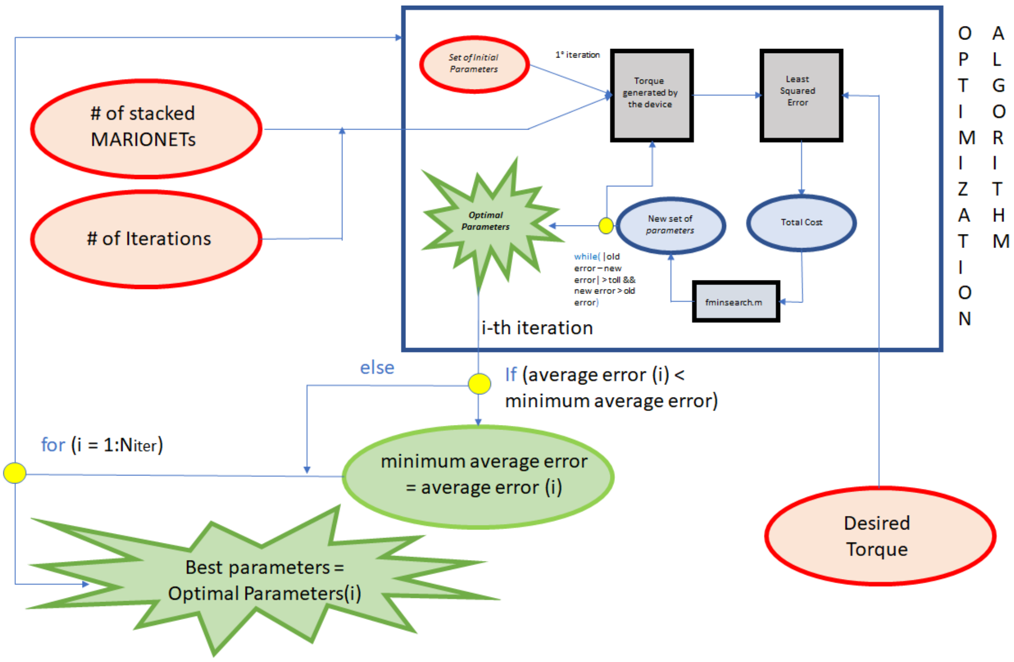

Figure 21: Flow chart of the developed algorithm.

To prove the fact that the results highly depend on the set of initial parameters, the average error for each i^{th} iteration is calculated and plotted, with $N_{iter} = 200$. Therefore, the trend of the error is shown and the maximum (*blue* circle) and the minimum(*green* circle) are highlighted; as the image points out, the error varies dramatically between different iterations with a variance $\sigma^2 = 0.0197$.

Figure 23 pictures what we previously noted: 23a displays the torque and error obtained with a set of parameters which is clearly non–optimal (*blue* circle of Figure 22), while 23b shows a successful run of the algorithm with a optimal set of parameters (*green* circle of Figure 22).

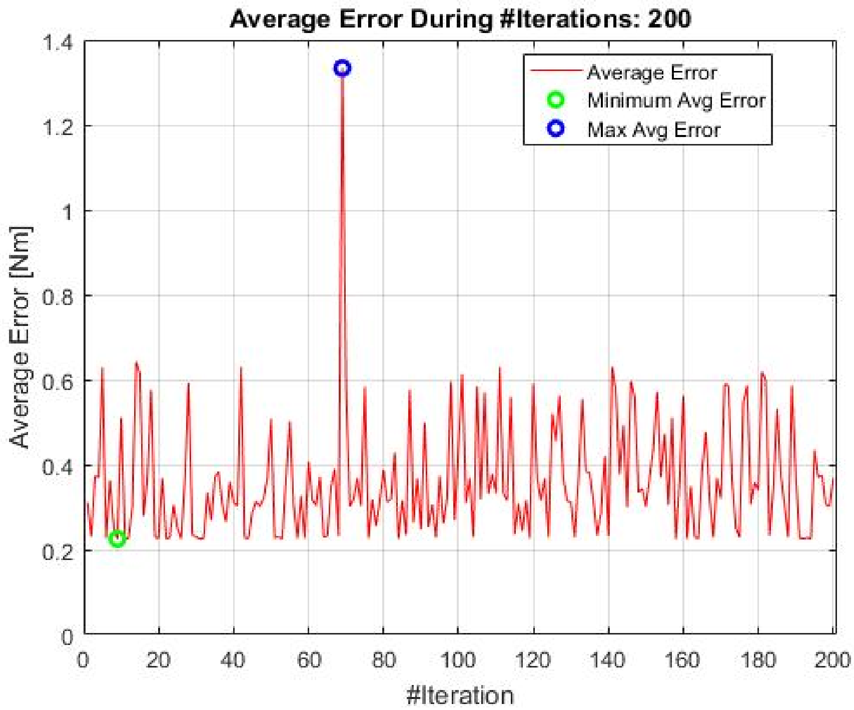

Figure 22: Average error for each iteration.

These results demonstrate the need for multiple iterations of the optimization algorithm and, moreover, it suggests that one can successfully find a globally optimal solution to the problem.

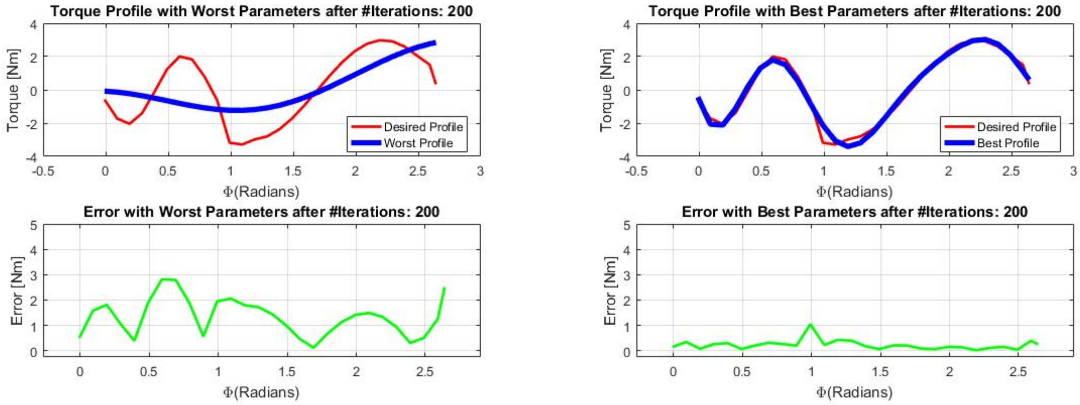

(a) Torque and error obtained with non–optimal parameters

(b) Torque and error obtained with optimal parameters

Figure 23: Comparison of the result of two different output of the algorithm.

3.2 Gravity compensation results

Here the results of the gravity compensation are presented, both in the form of the two one–joint and two–joints devices.

3.2.1 One–joint solution

The algorithm was run with the same specifications presented in section 3.1.1 for the elbow device, while the length of upper arm $L_{upper} = 0.35m$ was used for the shoulder device; in addition, a TBM $= 70Kg$ was chosen, so as to find the weight of the different parts of the arm using Equation 2.13–2.12. Moreover, in order to represent the vector field, the range of ϕ_1 ($\left[-\frac{\pi}{2}; 0\right]$) and the one of ϕ_1 ($\left[0; \frac{2\pi}{3}\right]$) were divided in 7 points, so as to have a total of 49 points in which the torques could be evaluated.

Running the algorithm, the two set of parameters were found. Moreover the absolute average error both in $[Nm]$ and [%] and the coefficient fo determination R^2 are calculated; R^2 is computed as:

$$R^2 = 1 - \frac{SS_{res}}{SS_{tot}} \tag{3.1}$$

being SS_{tot} is the sum of squared total and SS_{res} is the sum of squared residuals. This coefficient expresses the amount of variance explained by the model and it will be used in the next paragraphs as the discriminating factor to find the best and the worst approximations.

3.2.1.1 Elbow Device

In Table IV the average error, both in Nm and percentage, and the coefficient of determination are shown for the elbow joint, with the first column representing the fixed shoulder angles at which each torque profile is calculated. Some percentage errors are not reported because to be calculated they had to be divided by zero (Equation 3.2); in fact, being the target torque zero in some point and being

$$Err(\%) = |\frac{TargetTorque - OptimalTorque}{TargetTorque}| \times 100, \tag{3.2}$$

the resulting error would be $\approx \infty$, making it useless for any possible evaluation.

Moreover, in Table V the optimal parameters for the elbow device are reported.

As it can be noted, the error varies greatly throughout the overall space, from a minimum of $0.2493Nm(\approx 13\%)$ to a maximum of $1.0543Nm(\approx 139\%)$; this happens, probably, because the algorithm tries to approximate one of the profiles more than another leading to a great

TABLE IV: AVERAGE ERROR [Nm], AVERAGE ERROR [%] AND R^2 FOR EACH PROFILE FOR ELBOW TORQUE.

Shoulder Angle [rad]	Avg Abs. Error [Nm]	Avg Abs Error [%]	Coeff. of Determination
-1.5708	0.9819	—	-0.6198
-1.3090	0.6947	47.8814	-0.6330
-1.0472	0.4136	23.4124	0.0447
-0.7854	0.2493	13.1673	0.8178
-0.5236	0.3793	—	0.7629
-0.2618	0.6941	115.2472	0.5224
0	1.0543	139.5801	0.2127

TABLE V: OPTIMAL PARAMETERS FOR GRAVITY COMPENSATION AT THE ELBOW JOINT.

	R[m]	$\theta[rad]$
MARIONET1	0.0707	-0.2002
MARIONET2	0.0713	-2.1304
MARIONET3	0.0517	-4.2258
MARIONET4	0.0598	0.8025
MARIONET5	0.05	-1.3452

diversity in the performances. This can be simply perceived thanks to Figure 24 where the best and worst match are shown. In fact, in Figure 24a it can be seen that the two profiles are very similar both in the trend and in the magnitude (showing a $R^2 = 0.8178$), whereas in Figure 24b the two differs greatly in every aspect ($R^2 = -0.6198$); in fact, the calculated coefficient is negative, meaning that the resulting model behaves worst than how the mean would.

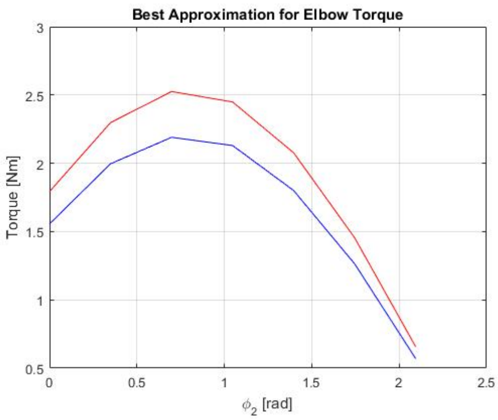

(a) Elbow torque corresponding to the best approximation.

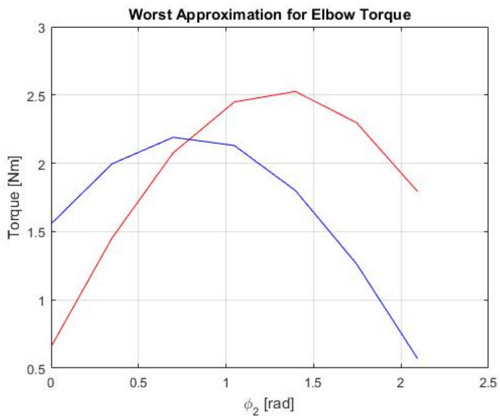

(b) Elbow torque corresponding to the worst approximation.

Figure 24: Elbow torques that are approximated in the best and worst way, respectively.

3.2.1.2 Shoulder Device

The process was repeated for the shoulder device; in Table VI the average errors are detailed for the shoulder joint. All the considerations previously made for the elbow device are still valid now for the shoulder equipment; the error, anyway, seems to be smaller with respect to the previous situation, with a minimum error of $0.4231Nm(\approx 9\%)$ and a maximum of $1.2167Nm(19,424\%)$ (unfortunately not presenting a percentage error for the aforementioned problem).

TABLE VI: AVERAGE ERROR [Nm] AND AVERAGE ERROR [%] FOR EACH PROFILE FOR SHOULDER TORQUE.

Elbow Angle [rad]	Avg Abs. Error [Nm]	Avg Abs Error [%]	Coeff. of Determination
0	0.9774	—	0.9188
0.3491	0.7186	20.5659	0.9450
0.6981	0.5683	6.8169	0.9580
1.0472	0.4826	8.7986	0.9691
1.3963	0.4231	9.1378	0.9599
1.7453	0.7246	12.5672	0.8388
2.0944	1.2167	19.424	0.4413

Furthermore, as in the elbow device case, the parameters for the shoulder device are shown in Table VII.

TABLE VII: OPTIMAL PARAMETERS FOR GRAVITY COMPENSATION AT THE SHOULDER JOINT.

	R[m]	$\theta[rad]$
MARIONET1	0.05	-0.4645
MARIONET2	0.0843	4.2597
MARIONET3	0.0957	2.7545
MARIONET4	0.0723	4.9682
MARIONET5	0.5	-0.0478

The same consideration that were done in the case of the elbow device are still valid for the shoulder system; in Figure 25 the best ($R^2 = 0.9691$) and the worst($R^2 = 0.4413$) approximation respectively are shown. What can be noted is that the obtained results seems to be quite satisfying for both the best and the worst case.

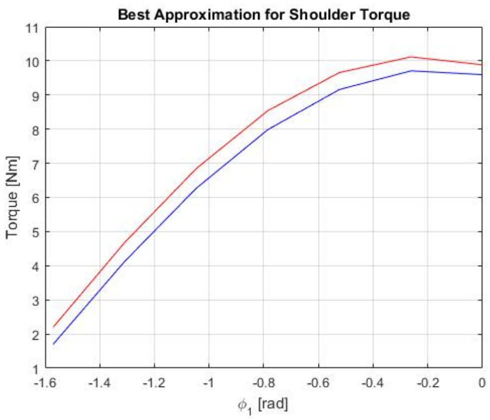

(a) Shoulder torque corresponding to the best approximation.

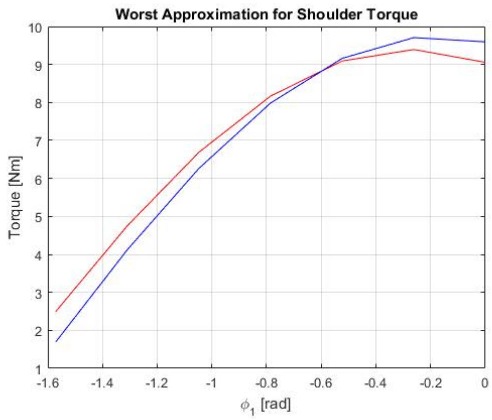

(b) Shoulder torque corresponding to the worst approximation.

Figure 25: Shoulder torques that are approximated in the best and worst way, respectively.

3.2.1.3 A specialized graphical display of results

Once the shoulder and elbow torque were obtained, they were converted into force using Equation 2.18, so as to picture a vector field as explained in section 2.5 and shown in Figure 26. The picture shows the vector field needed to compensate for gravity (in *red*) and the one obtained through the optimization algorithm (in *black*); it can be noted that the optimization seems to work better and better as the shoulder angle increases. Furthermore, the obtained torques do not results in a satisfying approximation especially for the most extreme points (for example, those where the arm is completely stretched).

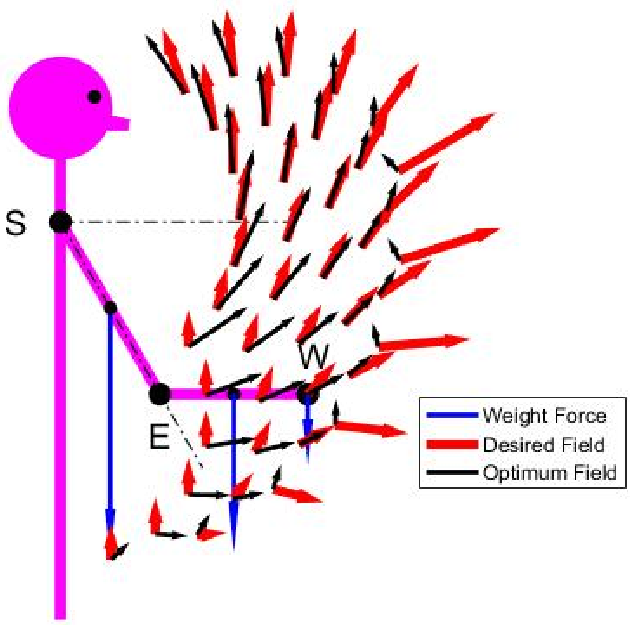

Figure 26: Vector field that we want to achieve (in *red*) and optimal field obtained with the algorithm (in *black*).

3.2.2 A MARIONET crossing two joints

The solution implementing the two–joints method is, finally, applied to the gravity compensation problem; the specification are the same as in section 3.1.1 except for the resting length of the spring that was set to be $L_0 = 0.4m$, longer than the previous case, since it has to link two points that are more distant than before. Figure 27 shows the arrangement of the two–joint device compared to the one–joint version.

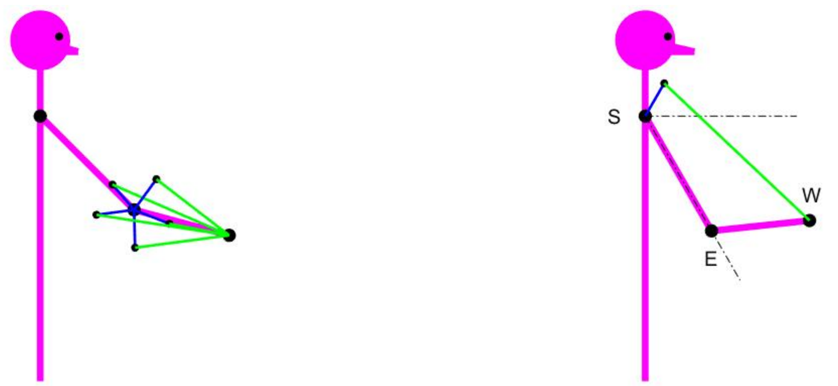

(a) One–joint MARIONET.

(b) Two–joint MARIONET.

Figure 27: Arrangement of a one–joint and two–joint MARIONETs.

Since only one optimal set of parameters had to be found taking into account both shoulder and elbow torque in the overall space, the results of a two–joint MARIONET by itself were expected to be highly non–satisfying.

As predicted, the obtained set of parameters was unable to suitably approximate the desired field needed to compensate for the weight of the arm. This was particularly true in the case of the torque at the elbow, as Figure 28 shows; in fact it can be seen that even where the error was at its minimum ($22.4681 Nm$) the MARIONET was not able to approximate nor the magnitude of the desired torque nor its trend (Figure 28a), as pointed out by the R^2 which is highly negative in this case. In Figure 28b the worst situation is pictured, showing a average error of $32.0597 Nm$.

Furthermore, the approximation of the shoulder torque (depicted in **??**)is still unsatisfying; in the best case, in fact, the average error is $6.0210 Nm$ (Figure 28c), while in the worst one it reaches $20.0612 Nm$(Figure 28d), with an $R^2 = -11.3297$ in the best case, which means that the model is completely not suited to approximate the desired torque field.

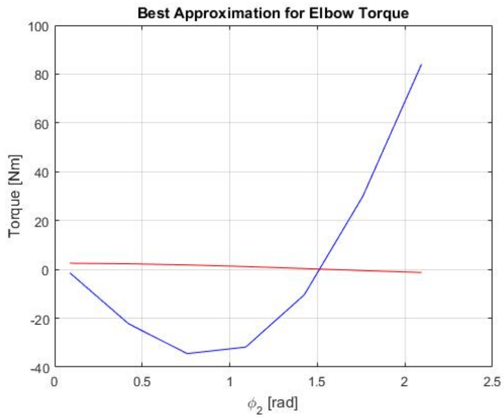

(a) Elbow torque corresponding to the best approximation for the two–joint case.

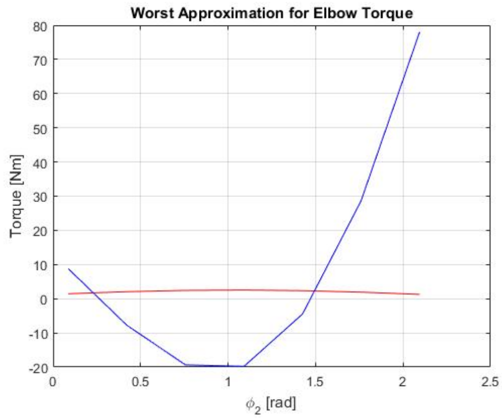

(b) Elbow torque corresponding to the worst approximation for the two–joint case

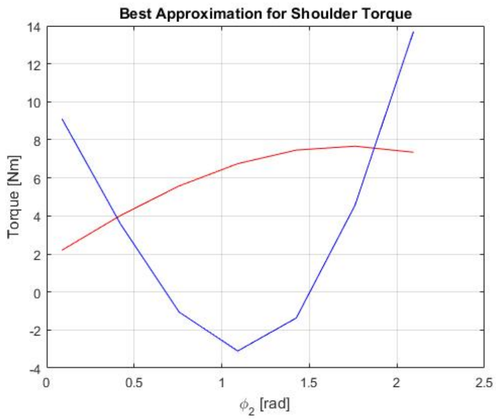

(c) Shoulder torque corresponding to the best approximation for the two–joint case.

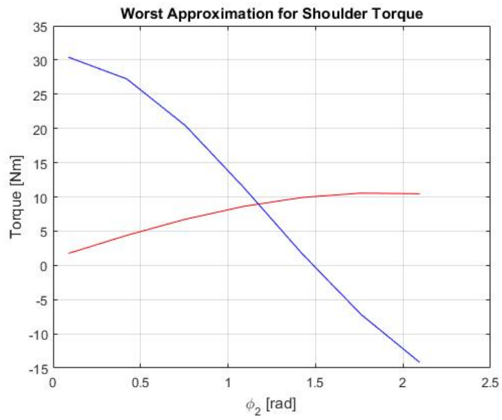

(d) Shoulder torque corresponding to the worst approximation for the two–joint case

Figure 28: Attempts to cancel gravity: the large amount of error suggests that a two–joint MARIONET by itself cannot provide adequate gravity cancellation (color convention match previous figures).

Finally, Figure 29 shows the desired vector field (*red*) and the one obtained thorough the algorithm implementing the two–joints solution; as previously noted, the overall resolution is clearly non–optimal and the picture strengthen the certainty.

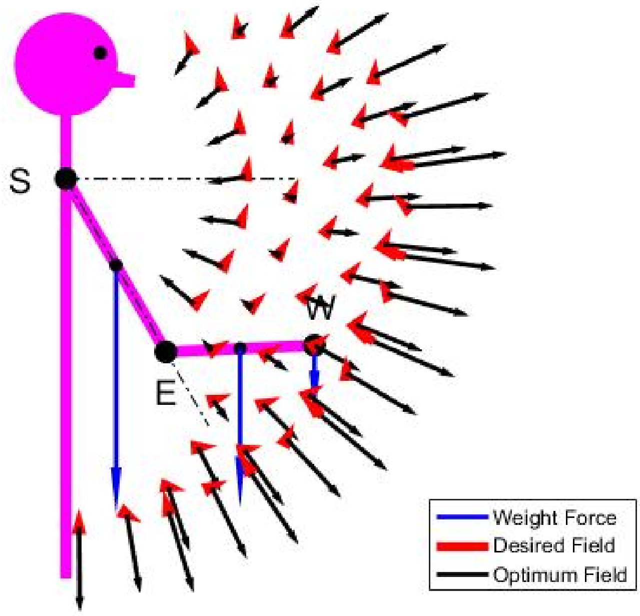

Figure 29: Vector field that we want to achieve (in *red*) and optimal field (in *black*) as obtained through the two–joints version of the algorithm; adequate gravity cancellation appears to be difficult with this mechanism by itself.

CHAPTER 4

CONCLUSIONS AND FUTURE DEVELOPMENT

More and more people in need for rehabilitation, a necessary tool for restoration of the functional capacity. In order to meet this compelling need, robotic devices not only to facilitate and accelerate rehabilitation, but also achieve better results where previous therapies failed.

The MARIONET is a simple mechanism able to exert customized torque profiles to the patient's limbs by adjusting the moment arm in order to obtain torque. Here, the MARIONET is expanded so as to obtain a portable system, completely passive and customizable to the needs and disabilities of the patient patient. Not only this device is thought to fit into a large variety of anthropometric dimensions, but also to achieve different tasks, such as assistance, error augmentation and gravity compensation.

Since a MARIONET is able to exert a sinusoidal torque field, the possibility of "stacking" a certain number of devices is taken into account so as to obtain more complex torques; this concept is similar to a truncated Fourier Transform, with each mechanism acting as a basis function.

The ability to achieve complicated torque profiles and the possibility to tune each single element according to certain specifications led to development of an optimization algorithm able to compute a set of optimal parameters which, in turn, could be used to customize the device on the patient's need.

This algorithm was proven to be able to obtain interesting outcomes resulting in the approximation of the different target profiles with which it was fed. The method was not only tested on "hand–made" torque profiles, but also on the moments generated by a person's muscles and whose aim is to compensate the weight of the human arm.

Different versions of the algorithm, corresponding to as many adaptations of the device, were developed and were able to evaluate one–joint or two–joints mechanism or to compute two or three parameters for each stacked elements. The one–joint version with two parameters resulted the best solution to approximate torque fields, presenting the lower computational work and the smaller time to process, despite a slightly worst error with respect ot the three parameters version. Furthermore, for what concerns the number of stacked MARIONETs the trade–off between the error and the comfort of the user resulted in five or six elements composing the total device. Finally, the two–joints version alone resulted to be not suited to achieve gravity compensation, while with the two single joint devices the approximation seems more satisfying.

The works that remains to do will be focused on the actual design and physical realization of the MARIONET device (Figure 30) and a clinical trial able to assess the real possibilities of the described mechanism. More work will be done on the optimization algorithm to make it more efficient , leading to the opportunity of using the more complex versions. For the gravity compensation problem, more work should be done so as to integrate two–joints and one–joint mechanism in the same device, so as to obtain more satisfying results. Furthermore, since the resting length and stiffness of the springs seems to have a strong impact on the final approximations, a version of the algorithm should be designed so as to implement those specifications as parameters. Finally, since in order to use MATLAB a highly expensive license is needed, the idea of writing the code in open languages such as *Python* will be taken into account enabling a larger usage of the algorithm.

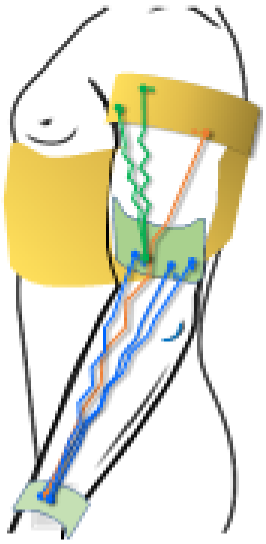

Figure 30: A possible design of the MARIONET.

CITED LITERATURE

1. Mozaffarian, D. e. a.: Heart disease and stroke statistics–2016 update. Circulation, 133:e38–e360, 2016.

2. Roger, V. L. e. a.: Heart disease and stroke statistics–2012 update. Circulation, 125:e2–e220, 2012.

3. Kelly-Hayes, M., Beiser, A., Kase, C. S., Scaramucci, A., DAgostino, R. B., and Wolf, P. A.: The influence of gender and age on disability following ischemic stroke: the framingham study. Journal of Stroke and Cerebrovascular Diseases, 12(3):119 – 126, 2003.

4. Foti, D., Pedretti, L. W., and Lillie, S. M.: Activities of daily living. Occupational therapy: Practice skills for physical dysfunction, pages 463–506, 1996.

5. G Thrift, A., Thayabaranathan, T., Howard, G., J Howard, V., M Rothwell, P., Feigin, V., Norrving, B., Donnan, G., and Cadilhac, D.: Global stroke statistics. 12, 10 2016.

6. Sturm, J., Donnan, G., Dewey, H., Macdonell, R., Gilligan, A., Srikanth, V., and Thrift, A.: Quality of life after stroke: the north east melbourne stroke incidence study (nemesis). Stroke, 35(10):2340 – 2345, 2004.

7. Tatemichi., T. K., Desmond, D. W., Stern, Y., Paik, M., Sano, M., and Bagiella, E.: Cognitive impairment after stroke: frequency, patterns, and relationship to functional abilities.

8. Bays, C. L.: Quality of life of stroke survivors: a research synthesis. 2001.

9. Rigby, H., Gubitz, G., Eskes, G., Reidy, Y., Christian, C., Grover, V., and Phillips, S.: Caring for stroke survivors: Baseline and 1-year determinants of caregiver burden. International Journal of Stroke, 4(3):152–158, 2009. PMID: 19659814.

10. Murie-Fernndez, M., Irimia, P., Martnez-Vila, E., Meyer, M. J., and Teasell, R.: Neurorehabilitation after stroke. Neurologa (English Edition), 25(3):189 – 196, 2010.

CITED LITERATURE (continued)

11. Volpe, B., Krebs, H., Hogan, N., Edelstein, L., Diels, C., and Aisen, M.: A novel approach to stroke rehabilitation. Neurology, 54(10):1938–1944, 2000.

12. Krebs, H. I., Aisen, M. L., Volpe, B. T., and Hogan, N.: Quantization of continuous arm movements in humans with brain injury. Proceedings of the National Academy of Sciences, 96(8):4645–4649, 1999.

13. Lum, P. S., Burgar, C. G., der Loos, M. V., Shor, P. C., Majmundar, M., and Yap, R.: The mime robotic system for upper-limb neuro-rehabilitation: results from a clinical trial in subacute stroke. In 9th International Conference on Rehabilitation Robotics, 2005. ICORR 2005., pages 511–514, June 2005.

14. Mazzoleni, S., Sale, P., Franceschini, M., Bigazzi, S., Carrozza, M. C., Dario, P., and Posteraro, F.: Effects of proximal and distal robot-assisted upper limb rehabilitation on chronic stroke recovery. 33, 06 2013.

15. Hornby, T. G., Campbell, D. D., Kahn, J. H., Demott, T., Moore, J. L., and Roth, H. R.: Enhanced gait-related improvements after therapist- versus robotic-assisted locomotor training in subjects with chronic stroke. Stroke, 39(6):1786–1792, 2008.

16. Marchal-Crespo, L. and Reinkensmeyer, D. J.: Review of control strategies for robotic movement training after neurologic injury. Journal of NeuroEngineering and Rehabilitation, 6(1):20, Jun 2009.

17. Fasoli, S., I Krebs, H., Stein, J., Frontera, W., and Hogan, N.: Effects of robotic therapy on motor impairment and recovery in chronic stroke. 84:477–82, 04 2003.

18. Emken, J. L., Benitez, R., and Reinkensmeyer, D. J.: Human-robot cooperative movement training: Learning a novel sensory motor transformation during walking with robotic assistance-as-needed. Journal of NeuroEngineering and Rehabilitation, 4(1):8, Mar 2007.

19. Vanderborght, B., Albu-Schaeffer, A., Bicchi, A., Burdet, E., Caldwell, D. G., Carloni, R., Catalano, M., Eiberger, O., Friedl, W., Ganesh, G., Garabini, M., Grebenstein, M., Grioli, G., Haddadin, S., Hoppner, H., Jafari, A., Laffranchi, M., Lefeber, D., Petit, F., Stramigioli, S., Tsagarakis, N., Van Damme, M., Van Ham, R., Visser, L. C., and Wolf, S.: Variable impedance actuators: A review. Robot. Auton. Syst., 61(12):1601–1614, December 2013.

CITED LITERATURE (continued)

20. Lee, J. H., Wahrmund, C., and Jafari, A.: A novel mechanically overdamped actuator with adjustable stiffness (mod-awas) for safe interaction and accurate positioning. Actuators, 6(3), 2017.

21. Sulzer, J. S., Peshkin, M. A., and Patton, J. L.: Marionet: An exotendon-driven rotary series elastic actuator for exerting joint torque. In 9th International Conference on Rehabilitation Robotics, 2005. ICORR 2005., pages 103–108, June 2005.

22. Sulzer, J., Peshkin, M., and Patton, J.: Design of a mobile, inexpensive device for upper extremity rehabilitation at home, pages 933–937. 12 2007.

23. Surdilovic, D., Bernhardt, R., Schmidt, T., and Zhang, J.: String-man: A new wire robotic system for gait rehabilitation. pages 64–67, 2003.

24. Levin, S. E., E, D., Perspective, H., and Of, S.: Raibert, m. h., ”legged robots that balance.” cambridge, mass.: Mit press (1986)., 1995.

25. Abdollahi, F., Lazarro, E. D. C., Listenberger, M., Kenyon, R. V., Kovic, M., Bogey, R. A., Hedeker, D., Jovanovic, B. D., and Patton, J. L.: Error augmentation enhancing arm recovery in individuals with chronic stroke: A randomized crossover design. Neurorehabilitation and Neural Repair, 28(2):120–128, 2014. PMID: 23929692.

26. Patton, J. and Huang, F.: Sensory-motor interactions and error augmentation, pages 79–95. Springer International Publishing, 1 2016.

27. Hsu, L. C., Wang, W. W., Lee, G. D., Liao, Y. W., Fu, L. C., and Lai, J. S.: A gravity compensation-based upper limb rehabilitation robot. In 2012 American Control Conference (ACC), pages 4819–4824, June 2012.

28. Prange, G. B., Stienen, A. H. A., Jannink, M. J. A., van der Kooij, H., IJzerman, M. J., and Hermens, H. J.: Increased range of motion and decreased muscle activity during maximal reach with gravity compensation in stroke patients. In 2007 IEEE 10th International Conference on Rehabilitation Robotics, pages 467–471, June 2007.

29. Sanchez, R. J., Liu, J., Rao, S., Shah, P., Smith, R., Rahman, T., Cramer, S. C., Bobrow, J. E., and Reinkensmeyer, D. J.: Automating arm movement training following severe stroke: Functional exercises with quantitative feedback in a gravity-reduced environment. IEEE Transactions on Neural Systems and Rehabilitation Engineering, 14(3):378–389, Sept 2006.

CITED LITERATURE (continued)

30. MathWorks: fminsearch.m, documentation.

31. de Leva, P.: Adjustments to zatsiorsky-seluyanov's segment inertia parameters. Journal of Biomechanics, 29(9).

VITA

NAME:	Tommaso Carella
EDUCATION:	Bachelor of Science in Biomedical Engineering, Politecnico di Milano, Milan, Italy, 2013−2016
	Master of Science in Biomedical Engineering, Politecnico di Milano, Milan, Italy, 2016−*Present*
	Master of Science in Bioengineering, University of Illinois at Chicago, Chicago, 2017−*Present*
EXPERIENCE:	Graduate Research Assistant in the Robotics Lab, Richard and Loan Hill Department of Bioengineering, University of Illinois at Chicago, Chicago, Gen 2018−*Present*